

Dielectric and interaction behavior of chitosan/polyvinyl alcohol and chitosan/polyvinyl pyrrolidone blends with some antimicrobial activities

T.H.M. Abou-Aiad^{a,*}, K.N. Abd-El-Nour^a, I.K. Hakim^a, M.Z. Elsabee^b

^aMicrowave Physics Department, National Research Centre, Cairo, Egypt

^bChemistry Department, Cairo University, Cairo, Egypt

Received 8 September 2004; received in revised form 4 February 2005; accepted 5 February 2005

Available online 22 November 2005

Abstract

The blends of chitosan, polyvinyl alcohol and chitosan polyvinyl pyrrolidone in dilute acetic acid were found to be compatible by viscosity measurements. The dielectric behavior of the investigated blends were studied using frequency response analyzer covering a frequency range from 10^2 to 10^6 Hz and in a wide range of temperature. The permittivity ϵ' was found to decrease by increasing the frequency showing an anomalous dispersion. The dielectric loss ϵ'' data on the frequency domain were found to be broad indicating that more than one relaxation mechanism is present. The data for the whole investigated systems were fitted using Fröhlich and/or Havriliak–Negami functions in addition to the conductivity term. The function detected below T_g could be ascribed to an orientation movement related to the side chain. A second function in the lower frequency range could be ascribed as a Maxwell Wagner effect which arises from the interfacial polarization caused by the multi-constituents of the investigated systems.

The biological activity of such investigated systems was tested against a representative number of pathogenic organisms by determining the minimum inhibitory concentration (MIC). The activity was found to increase by increasing the amount of CS in the blend.

© 2005 Elsevier Ltd. All rights reserved.

Keywords: Chitosan; PVA; PVP

1. Introduction

Chitosan is a deacetylated product of chitin, a natural polymer, which is obtained from the cuticle of the marine crustaceans such as crabs and shrimps. Both chitin and chitosan have been widely investigated for the last two decades due to their industrial and biomedical applications [1,2]. In addition, chitosan is expected to be useful in the development of composite materials such as blends with other polymers, since chitosan has many functional groups [3,4]. Polymer–polymer miscibility is a very significant factor especially for mechanical property of the blend. This miscibility is generally considered as a result of specific interaction between the polymer segments [5–14]. Blends of

chitosan with several polymers have attracted much scientific interest, for example CS/polyacrylic acid membranes blends were prepared for water–ethanol separation, it was found that all these membranes are highly water-selective [15]. Polytetrafluoroethylene used in large diameter blood vessels exhibits marked reduction in platelets formation upon chemical modification of its surface with CS/PVA blends [16]. The mechanical and dielectrical properties of beta chitin/PVA blends were examined and were shown to be miscible [17]. Polymer interactions in polyamide 6/CS blends have been investigated by FTIR [18]. Blends of CS/PVP appeared to be clear on appearance. IR spectra indicated the carbonyl–OH hydrogen bonding between chain–chain in the blend and consequently their compatibility [19]. CS/PVA blends were shown to exhibit anti-bacterial activity but no anti-fungal activity [20]. Mechanical and DSC analysis suggested partial miscibility of CS/viscose rayon blends [21].

The aim of this work is to study molecular interactions between chitosan when blended with PVA and PVP using the viscosity measurements. The relaxation mechanisms of such systems were also investigated through the dielectric

* Corresponding author. Address: Microwave Physics, Physics Division, National Research Centre, Elbehos St Gizza, Room: 12, Gizza 12622, Egypt. Tel.: +20 2 3371344; fax: +20 2 3370931.

E-mail address: tamany22@yahoo.com (T.H.M. Abou-Aiad).

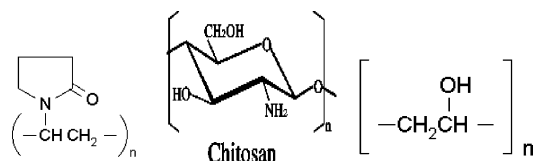
measurements. The biological activity will be tested against a representative number of pathogenic organisms.

2. Experimental part

2.1. Materials used

Chitosan with a degree of deacetylation of 78% and an average molecular weight of $3\text{--}4 \times 10^5$, poly(*N*-vinyl-2-pyrrolidone) PVP with an average molecular weight of 4×10^5 and polyvinyl alcohol PVA with degree of deacetylation 99%, and an average molecular weight 1.25×10^5 were supplied by Aldrich, Germany.

The solvents, and acetic acid were of analytical grade from commercial sources and used without further purification.



Poly (N-Vinyl-2-pyrrolidone) PVP

Polyvinyl alcohol PVA

2.2. Preparation of the blends

Chitosan, PVP and PVA in 1 wt% aqueous acetic acid were mixed in different ratios. Solutions of different compositions were poured on a glass plate that was prior brushed with cotton saturated by ethanol and evaporated at room temperature. The thickness of the obtained membrane was about 30 μm .

2.3. Measurements of the viscosity

All measurements were performed at $(20 \pm 0.1 \text{ }^\circ\text{C})$ with an Avs 350 automatic Ubbelohde-type capillary viscometer from Schott-Geraete (Hofheim, Germany) which allows reproduction of the flow times with an accuracy of 0.03 s. The instrument was also equipped with a model CT 1450 thermostated bath.

The solution of binary system was prepared by dissolving the polymer blend in 1 wt% aqueous acetic acid up to a concentration of 1 g/100 ml. Dilution to yield at least five lower concentrations were made by adding the appropriate aliquots of solvent. The elution time of each solution is then determined as the average of four readings. The intrinsic viscosity was determined from the Huggin's plots [22] of the relative viscosity versus concentration by the extrapolation to infinite dilution (zero solute concentration).

2.4. Measurements of the permittivity and dielectric loss in the frequency range $10^2\text{--}10^6$ Hz

Measurements of the permittivity and dielectric loss of the investigated samples prepared by casting method were carried out in the frequency range from 10^2 to 10^6 Hz. The dielectric apparatus contains a frequency response analyzer (Schlumberger solartron 1260), an electrometer amplifier, some relays, resistors, condensers and measuring cell.

2.5. Biological activity

The activity of the prepared blends was tested by minimum inhibitory concentration (MIC) method [32]. MIC was determined by diluting the agent where the filter paper discs were impregnated with the diluted samples.

The micro-organisms used were *E. coli* (1357), *B. sereur* (1080), *B. subtilis* (1020), *P. aeruginosa* (1259), *Aspergillus niger* (147), and *Candida albicans* (22) and obtained from Microbiological Resource Centre (MIRCEN).

3. Results and discussion

3.1. Viscosity measurements

The viscometric technique was applied to investigate the miscibility of polymeric blends in solution. The nature of the viscosity of dilute polymer solutions is based on analysis of their hydrodynamic properties, that is, properties related to the movement of macromolecules in solution. The two phase structures of polymer mixtures and the deformation of the drops in flow may affect the value of viscosity. For this reason, the effective viscosity of a polymer mixture depends not only on the component ratio but also on the value of viscosity. The principle of using dilute solution viscosity to measure the miscibility characterization is based on the fact that, while in solution, molecules of both components may exist in a molecularly dispersed state, and they undergo a natural attraction or repulsion that will influence the viscosity.

For a ternary system formed by polymer (1), polymer (2), and solvent (3), the intrinsic viscosity of the mixture $[\eta]_m$ denotes the coil dimensions, which can be altered by contraction or expansion of the coil, whether the interactions between unlike polymer segments are attractive or not. Likewise, the viscometric interaction parameter (b_m) characterizes the overall interaction between like chains of both polymers and can be used to determine polymer–polymer compatibility. With the previous assumption, these two criteria of polymer–polymer compatibility are based on the classical Huggins's equation [22].

$$\eta_{sp} = [\eta]C + k[\eta]^2C^2 \quad (1)$$

where the specific viscosity η_{sp} of the single solute solution was expressed as a function of the concentration C , and $[\eta]$

is the intrinsic viscosity, with the assumption that $k[\eta]^2 = b$, where b reflects the binary interaction between polymer segments. Eq. (1) can be expressed in a weight-average form because the reduced viscosity is an additive property

$$\frac{(\eta_{sp})_m}{C_m} = \sum \frac{(\eta_{sp})_i w_i}{C_i} \quad (2)$$

with $w_i = C_i/C_m$ is the weight fraction of polymer i , combination of Eqs. (1) and (2) gives

$$\begin{aligned} \frac{(\eta_{sp})_m}{C_m} &= \sum ([\eta]_i + b_i C_i) w_i \\ &= \sum [\eta]_i w_i + C_m \left(\sum b^{1/2} w_i \right)^2 \end{aligned} \quad (3)$$

comparing Eqs. (1)–(3) one gets

$$[\eta]_m = \sum [\eta]_i w_i \text{ and } b_m = \left(\sum b^{1/2} w_i \right)^2 \quad (4)$$

The intrinsic viscosities for the ternary system (CS/PVA/CH₃COOH·H₂O) measured at 20 °C were obtained from the extrapolation of the Huggins's equation for all the investigated compositions of the blends. These intrinsic viscosities are shown graphically in Fig. 1. From this figure, it is clear that the intrinsic viscosities of the different compositions reflect the change in the molecular dimensions of CS and PVA as a result of interactions between unlike chains.

Moreover, the slopes of the lines from Huggins's plot that predicts the interaction parameters b_m are shown graphically

in Fig. 1. The change in the values of these slopes reflects the interaction between the polymer–polymer compositions.

In order to study the interaction between both polymers in the system and to give a useful insight about the attractive and repulsive molecular interaction, three different criteria were used. These three different parameters ($\Delta[\eta]$, Δb and $\Delta b'$) were calculated for the investigated system and the data obtained are shown graphically in Fig. 2.

These criteria were based on the difference between the experimental and ideal values of either the intrinsic viscosity or the interaction parameter

$$\Delta[\eta]_m = [\eta]_m^{\text{exp}} - [\eta]_m^{\text{id}} \quad (5)$$

where $[\eta]_m^{\text{exp}}$ is determined from the extrapolation of the Huggin's equation and $[\eta]_m^{\text{id}}$ is obtained from the data of the individual polymers

$$[\eta]_m^{\text{id}} = [\eta]_1 w_1 + [\eta]_2 w_2 \quad (6)$$

where w_1 , w_2 are the weight fractions of polymer 1 and polymer 2, respectively. The difference between the experimental and the ideal values of the interaction parameter $\Delta b_m = b_m^{\text{exp}} - b_m^{\text{id}}$ can be used to discuss the miscibility of the polymer blend solutions. The ideal value of the global viscometric interaction parameter b_m^{id} is calculated from

$$b_m^{\text{id}} = b_1 w_1^2 + b_2 w_2^2 + 2(b_1 b_2)^{1/2} w_1 w_2 \quad (7)$$

where, b_m^{exp} is obtained from the Huggin's plots as indicated previously. The summation in Eq. (3) is a mathematical

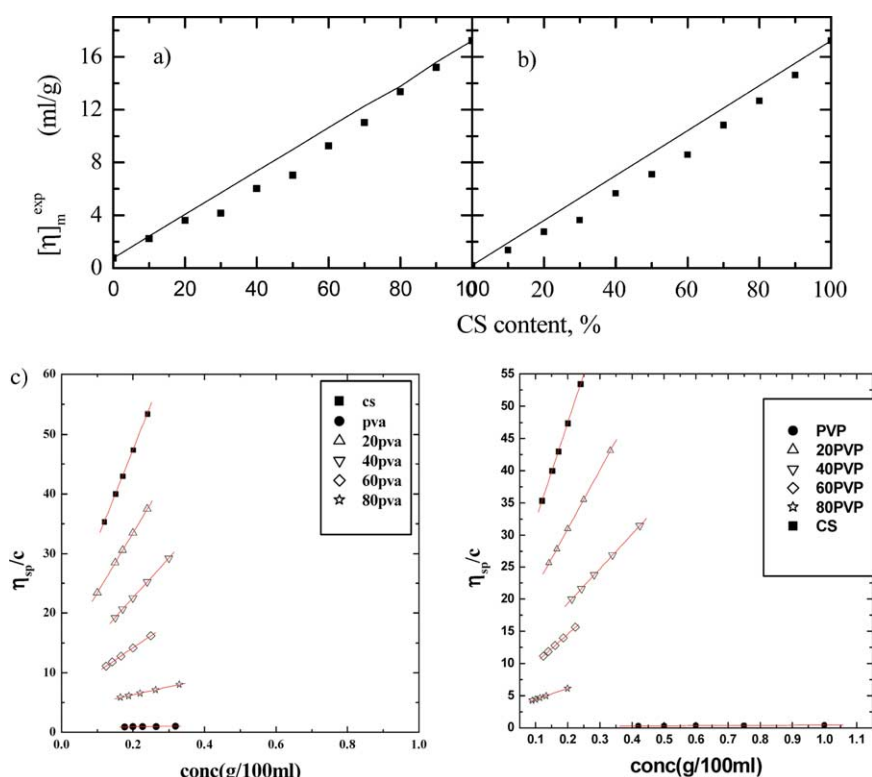


Fig. 1. Intrinsic viscosity dependence on blend content (a) CS/PVA, (b) CS/PVP, (c) Huggin's plots (reduced viscosity in relation to the polymer concentrations).

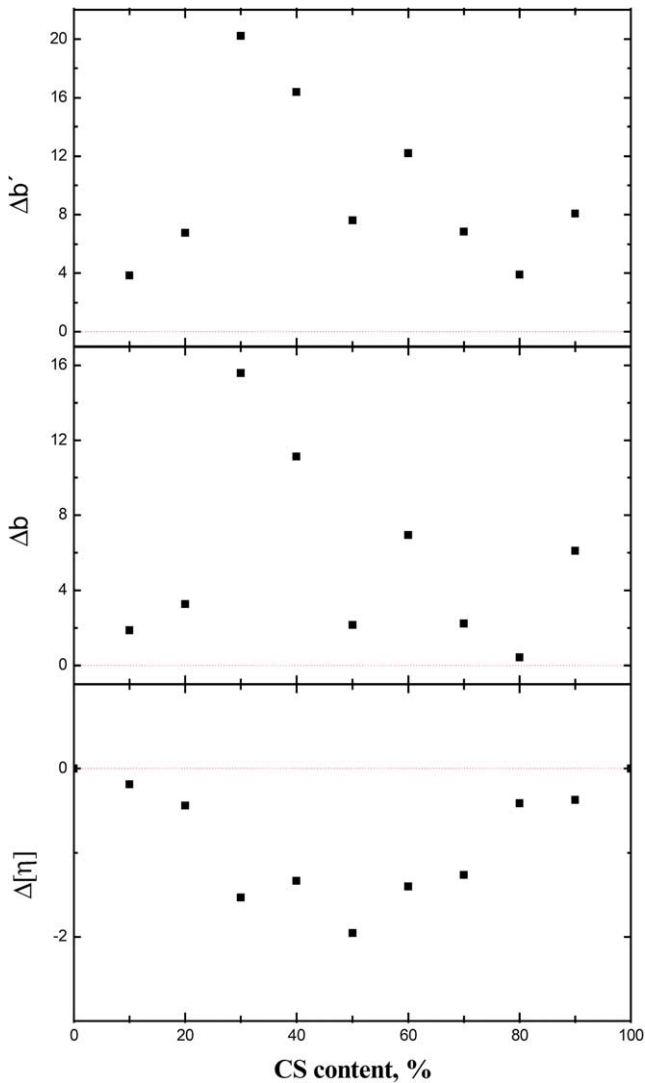


Fig. 2. Plots of different compatibility magnitudes (Δ s) as a function of mixture composition for the polymer blend CS/PVA (the system was compatible as $\Delta\eta < 1$ and Δb and $\Delta b' > 1$).

mistake, which exists by development of the summation of the second term:

$$\sum b_i w_i^2 = \sum (b^{1/2} w_i)^2 \quad (8)$$

For this reason, a new viscometric interaction parameter b_m^{id} was developed and is given by

$$b_m^{\text{id}} = b_1 w_1^2 + b_2 w_2^2 \quad (9)$$

This new parameter can be used in addition to b_m .

From Fig. 2, the values of three delta parameters ($\Delta[\eta]$, Δb and $\Delta b'$) for the different compositions change from positive to negative signs, reflecting the degree of compatibility of the system. Comparing these data with those found by Garcia [23,24] for (PES/PVDF), it is concluded that (CS/PVA/CH₃COOH·H₂O) is compatible. As the system was compatible when $[\eta]_m^{\text{exp}} < [\eta]_m^{\text{id}}$ and $b_m^{\text{exp}} > b_m^{\text{id}}$

where as it was considered incompatible when $[\eta]_m^{\text{exp}} > [\eta]_m^{\text{id}}$ and $b_m^{\text{exp}} < b_m^{\text{id}}$.

Viscosity behavior has been also studied for the ternary system (CS/PVP/CH₃COOH·H₂O). The reduced viscosity for both individual polymers and their compositions has been conducted and their plots against the concentration of the mixture are fitted through the Huggins's equation. The intrinsic viscosities as well as the viscometric interaction parameters for this system and their assayed compositions at 20 °C are compiled in Fig. 3.

From these figures it is important to notice that (CS/PVP/CH₃COOH·H₂O) system in the whole composition range has a negative deviation from the theoretical or ideal line formed between both individual polymers (CS and PVP). Fig. 1(b) relating intrinsic viscosity and the composition for CS/PVP system shows that in all cases the intrinsic viscosity of the blend is lower than the average $[\eta]$ of the pure polymers. The deviation seen in this figure could be attributed to deviation from linearity of the free volume in the system. Free volume changes are related to the interactions between polymer chains, that reflects orientation effects. On the other hand, the negative deviation of $[\eta]$ from linearity given in case of CS/PVP, is found to be higher when compared with that of CS/PVA system (Fig. 1(a)), which can be considered as evidence for the existence of specific interaction between the hydroxyl group and the carbonyl group in the polymer blends. To investigate the degree of compatibility in this system, the three criteria which have been applied before in the case of (CS/PVA/CH₃COOH·H₂O) were also calculated, listed in Table 4. According to these data, it is found that this system (CS/PVP/CH₃COOH·H₂O) is compatible as $[\eta]_m^{\text{exp}} < [\eta]_m^{\text{id}}$ and $b_m^{\text{exp}} > b_m^{\text{id}}$.

3.2. Dielectric measurements

3.2.1. CS, PVA and PVP homopolymers

The permittivity ϵ' , dielectric loss ϵ'' and loss tangent $\tan \delta$ of CS, PVA and PVP were carried out at different frequencies ranging from 10² to 10⁶ Hz and different temperatures ranging from 30 to 190 °C. The values of ϵ' were found to increase by increasing temperature and decrease by increasing frequency showing an anomalous dispersion. The absorption curves relating ϵ'' and log frequency were found to be broad and increase by increasing temperature indicating that more than one relaxation mechanism is present. To study these mechanisms, the data for the three investigated homopolymers at the different temperatures were analyzed using a proper function. The data obtained from the analyses are given in Tables 1–3. Examples of the analyses are given in Fig. 4 for CS, PVA and PVP at 90 °C.

The data of CS was found to be fitted by Fröhlich [25] and Havriliak–Negami [26] functions plus the conductivity term.

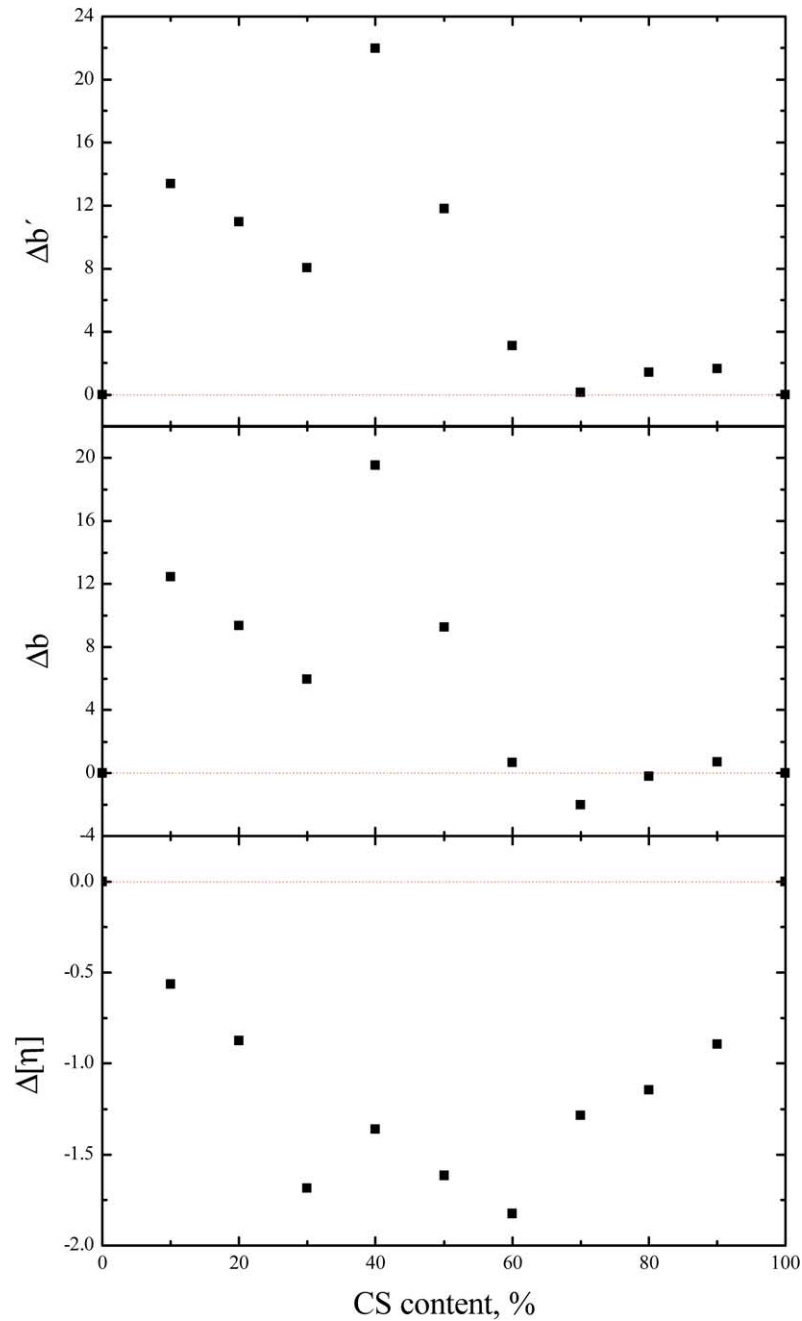


Fig. 3. Plots of different compatibility magnitudes (Δ s) as a function of mixture composition for the polymer blend CS/PVP (the system was compatible as $\Delta\eta < 1$ and Δb and $\Delta b' > 1$).

Table 1
Relaxation parameters using Havriliak–Negami (HN) and Fröhlich (F) functions of CS

Temperature (°C)	$\tau_F \times 10^4$ (s)	S_F	$\tau_{HN} \times 10^5$ (s)	S_{HN}	α	β	$\sigma \times 10^{10}$ (S/m)
50	8.91	1.353	9.08	1.382	0.20	0.46	1.06
70	8.91	2.527	6.59	1.987	0.20	0.44	3.03
90	8.91	2.976	4.42	2.289	0.24	0.57	6.34
110	8.91	5.681	3.08	2.871	0.24	0.55	12.50

τ_F and τ_{HN} are the Fröhlich and Havriliak–Negami relaxation time, S_F and S_{HN} are the relaxation strength, α and β the relaxation parameters and σ is the conductivity.

Table 2
Relaxation parameters using Havriliak–Negami (HN) function of PVP

Temperature (°C)	$\tau_{\text{HN}} \times 10^4$ (s)	S_{HN}	α	β	$\sigma \times 10^{12}$ (S/m)
30	8.56	0.083	0.27	0.28	1.25
50	6.73	0.110	0.30	0.34	1.84
70	4.88	0.161	0.31	0.40	2.79
90	5.51	0.148	0.33	0.39	2.15
110	3.84	0.217	0.39	0.50	3.03

τ_{HN} is Havriliak–Negami relaxation time, S_{HN} is the relaxation strength, α and β the relaxation parameters and σ is the conductivity.

Fröhlich function

$$\varepsilon^*(\omega) = \varepsilon_\infty + \frac{\varepsilon_s - \varepsilon_\infty}{\ln(\tau_1/\tau_2)} \ln \frac{\tau_1(1 + i\omega\tau_2)}{\tau_2(1 + i\omega\tau_1)}$$

Havriliak–Negami function

$$\varepsilon^*(\omega) = \varepsilon_\infty + \frac{\varepsilon_s - \varepsilon_\infty}{[1 + (\omega\tau)^{1-\alpha}]^\beta}$$

where ε_∞ is the permittivity at infinite frequency or is the optical permittivity, ε_s is the measured permittivity at low frequency or is the static permittivity and $\omega = 2\pi f$ (rad s⁻¹). Also the relaxation parameters must be $0 \leq \alpha, \beta \leq 1$.

Assuming a homogenous medium of conductivity σ (ohm⁻¹ cm⁻¹), the joule heating arising from the conductivity contributes a loss factor ε'' (conductance) so that the observed value at frequency f (Hz) is

$$\varepsilon''_{\text{total}} = \varepsilon''_{\text{dielectric}} + \varepsilon''_{\text{conductance}}$$

The first relaxation time τ_{F} in the lower frequency range which was fitted by Fröhlich function with distribution parameter $p=2$ could be attributed to Maxwell Wagner effect [27,28] as no detectable change in the relaxation time τ_{F} was noticed by increasing temperature. This affect could be due to the presence of a relatively high residual concentration of impurities attached to bulk of chitosan during the drastic hydrolysis of chitin.

The second relaxation time τ_{HN} which was fitted at the higher frequency range by Havriliak–Negami function and was found to decrease by increasing temperature could be attributed to a relaxation related to the side chain as the measurements were carried out at temperatures below the T_{g} of such polymer ($T_{\text{g}} \sim 225$ °C) [29]. The origin of such

relaxation is a partial rotation of the several side groups present in CS around the six members ring composing the main back-bone of the polymer. The orientation, which could be related to the main chain is expected to be frozen at that range of temperature. According to Arrhenius equation the activation energy corresponds to this relaxation process was calculated and was found to be 13 kJ mol⁻¹.

$$\tau(T) = A \exp\left(\frac{E_a}{k_{\text{B}}T}\right) \quad (10)$$

where A is a constant, E_a is the activation energy of the corresponding relaxation process and k_{B} is Boltzmann constant.

In case of PVP, the absorption curves at different temperatures were found to be fitted by HN function plus the conductivity term. The relaxation time τ_{HN} corresponds to this function is comparable with that of CS as it could ascribe the relaxation related to the side chain whose origin could be due to the rotation of the pyrrolidone group around the main chain of the polymer as the measurements were carried out at temperatures below that of its T_{g} ($T_{\text{g}} \sim 190$ °C) [29]. The activation energy for this process was calculated and found to be close to that of CS (12 kJ mol⁻¹).

For PVA where its glass transition ($T_{\text{g}} \sim 55$ °C) [30] is lower than those for CS and PVP, the dielectric measurements were carried out at a broader range of temperature covering both ranges below and above T_{g} . The absorption curves for such homopolymer were fitted at lower temperature by Havriliak–Negami and Fröhlich functions plus conductivity term while those at higher temperature were fitted by only Havriliak–Negami plus conductivity term. This could be attributed to the phase change, which

Table 3
Relaxation parameters using Havriliak–Negami (HN) and Fröhlich (F) functions of PVA

Temperature (°C)	$\tau_{\text{HN}} \times 10^3$ (s)	S_{HN}	α	β	$\tau_{\text{F}} \times 10^6$ (s)	S_{F}	$\sigma \times 10^{12}$ (S/m)
50	1.44	0.198	0.25	0.4	5.51	0.176	1.3
70	6.73	0.841	0.28	0.6	1.16	0.297	42.0
90	0.70	5.074	0.25	0.6	0.41	0.484	138.0
110	1.69	34.170	0.10	0.9	0.87	1.233	1790.0
130	1.05	336.700	0.10	1.0	–	–	8870.0
150	0.70	1505.000	0.10	1.0	–	–	24100.0
170	0.59	3659.000	0.10	1.0	–	–	51600.0
190	0.51	10090.000	0.10	1.0	–	–	56000.0

τ_{F} and τ_{HN} are the Fröhlich and Havriliak–Negami relaxation time, S_{F} and S_{HN} are the relaxation strength, α and β the relaxation parameters and σ is the conductivity.

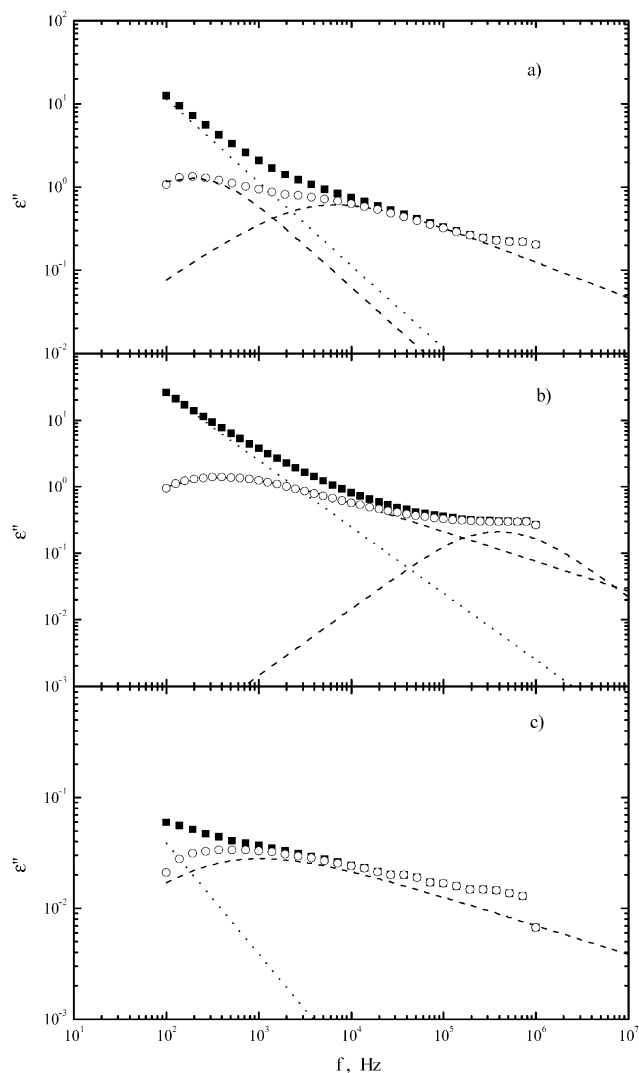


Fig. 4. Absorption curves of (a) CS, (b) PVA and (c) PVP at 90 °C. The data are fitted by one Havriliak–Negami, one Fröhlich and conductivity term. (■) ϵ''_{exp} , (---) ϵ''_{HN} , (○) ϵ''_{theo} , (- - -) ϵ''_{F} , (···) ionic conductivity.

could take place at the glass transition temperature. At higher temperature, the relaxation mechanism which was characterized by the relaxation time τ_{HN} could be attributed to the orientation of the main chain. This orientation is associated with the glass transition temperature and assign to micro-Brownian motion. The activation energy of such process was calculated and was found to be (25 kJ mol⁻¹). In that range of temperature no indication for the relaxation, which could be ascribed to the orientation of the side chain. At lower temperatures the data which was found to be fitted by Fröhlich function with distribution parameter ($P=2$) and was expected to ascribe such mechanism is comparable with that found before [31] at a lower range of temperature (less than 20 °C).

The activation energy for such process was also calculated and found to be close to those for CS and PVP (13 kJ mol⁻¹).

The dielectric strength related to the number of dipolar units involved in the measured relaxation processes and

evaluated from the maximum of the dielectric loss peak results for both processes S_{F} and S_{HN} given in Tables 1–3 were found to increase by increasing temperature.

The conductivity data given in Tables 1–3 for the three investigated homopolymers indicate that CS has conductivity higher than that of PVP at the whole temperature range. These conductivities were found to increase by increasing temperature due to the increase in the ionic mobility. This increase was found to be more pronounced in the case of PVA even its conductivity at 50 °C is similar to that of PVP.

3.2.2. CS/PVP and CS/PVA blends

The permittivity ϵ' , dielectric loss ϵ'' and loss tangent $\tan \delta$ for CS/PVP and CS/PVA with the different compositions (20, 50 and 80% CS) were carried out at different frequencies ranging from 10² to 10⁶ Hz and different temperatures ranging from 30 to 110 °C. From these figures, it is seen that ϵ' decreases by increasing frequency while it increases by increasing temperature. On the other hand, the broadness of the absorption curves detected in those figures indicates that more than one relaxation process is present. The ϵ'' data given for both blends with the different compositions at different temperatures were found to be fitted by Fröhlich and Havriliak–Negami functions plus the conductivity term. The data obtained from the analyses are given in Tables 4 and 5. Examples of the analyses are shown graphically in Figs. 4 and 5 for both blends with the different compositions at 90 °C. It is interesting to find that the first relaxation time τ_{F} in the lower frequency range which was fitted by Fröhlich function with distribution parameter $P=2$ could be attributed to Maxwell Wagner effect as no pronounced change in τ_{F} was noticed by increasing either the temperature or the composition of the blend. The origin of such effect is an Ac, which is in phase with the applied potential. These current are resulted from the difference in permittivity and receptivity of the blend components (Fig. 6).

The second relaxation time τ_{HN} which was fitted at the higher frequency range by Haveriliak–Negami function was found to decrease by increasing temperature. This relaxation process could be ascribed to an orientation related to the side chain as the measurements were carried out at temperature below the T_{g} (of the investigated compositions). This process is considered to be locally cooperative as the side chain movements imply some coordinate motion with the neighboring side chains of the other polymer. For such process, the activation energy for each composition was calculated and the data obtained indicate that these values are closed to each other and equal to (13–15 kJ mol⁻¹).

3.3. Biological activity measurements

The biological activity of the two investigated systems (CS/PVA and CS/PVP) were tested against a representative number of pathogenic organisms (*E. coli*, *B. sereur*, *B.*

Table 4
Relaxation parameters using Havriliak–Negami (HN) and Fröhlich (F) functions of CS/PVA

Temperature (°C)	$\tau_F \times 10^4$ (s)	S_F	$\tau_{HN} \times 10^5$ (s)	S_{HN}	α	β	$\sigma \times 10^{11}$ (S/m)
20% CS							
30	8.22	1.243	13.56	2.960	0.30	0.46	10.6
50	8.22	4.411	12.02	4.297	0.3	0.55	46.7
70	–	–	–	–	–	–	–
90	8.22	5.947	4.78	5.317	0.30	0.60	113.0
110	8.22	9.872	2.96	6.777	0.30	0.66	223.0
50% CS							
30	8.22	1.102	12.51	2.308	0.20	0.13	4.4
50	8.22	2.716	10.67	3.714	0.26	0.38	21.0
70	8.22	6.106	9.08	5.622	0.27	0.41	85.2
90	8.22	6.277	7.14	6.452	0.30	0.52	90.6
110	8.22	29.590	5.62	11.490	0.33	0.66	406.0
80% CS							
30	8.22	0.461	13.02	1.096	0.34	0.42	1.13
50	8.22	2.528	11.10	4.173	0.28	0.50	14.10
70	8.22	10.150	8.73	7.946	0.23	0.55	620.00
90	8.22	105.900	4.98	10.180	0.20	0.60	3130.00
110	8.22	180.900	3.48	15.760	0.17	0.65	7100.00

τ_F and τ_{HN} are the Fröhlich and Havriliak–Negami relaxation time, S_F and S_{HN} are the relaxation strength, α and β the relaxation parameters and σ is the conductivity.

subtilis, *P. aeruginosa*, *Aspergillus niger*, *Candida albicans*).

The monitoring of antimicrobial activity is usually performed by determination of the MIC [32], the smallest amount of the agent that inhibits the multiplication of the pathogen. The actual antimicrobial concentration is represented by the diameter of the zone of inhibition formed around the discs impregnated with the polymer in different composition ratios. Therefore, it is found that the MIC for

both systems decrease by increasing the amount of CS in the blends reaches 10^{-7} mg/l for CS while that for PVP was 10^{-3} mg/l in comparable with PVA while is considered to be biologically inactive.

The antimicrobial activity could be attributed to the diffusion of the polymers (antimicrobial polymers) which inhibit the growth of the micro-organism, i.e. an interaction between the antimicrobial agent and micro-organisms is taken place. The detection of this interaction is not only by

Table 5
Relaxation parameters using Havriliak–Negami (HN) and Fröhlich (F) functions of CS/PVP

Temperature (°C)	$\tau_F \times 10^4$ (s)	S_F	$\tau_{HN} \times 10^5$ (s)	S_{HN}	α	β	$\sigma \times 10^{11}$ (S/m)
20% CS							
30	8.56	0.813	12.51	0.664	0.31	0.40	2.72
50	8.56	1.384	8.73	0.941	0.30	0.50	4.06
70	8.56	0.784	6.59	0.664	0.30	0.56	2.61
90	8.56	0.715	5.62	0.664	0.30	0.64	2.61
110	8.56	1.017	4.25	0.871	0.35	0.66	3.19
50% CS							
30	7.29	1.260	6.86	0.959	0.30	0.41	0.756
50	7.29	1.332	5.39	1.922	0.30	0.57	4.060
70	7.29	2.339	4.42	3.059	0.30	0.53	14.100
90	7.29	1.878	5.62	3.903	0.26	0.70	15.200
110	7.29	3.059	7.44	3.809	0.26	0.70	14.100
80% CS							
30	8.22	1.157	8.06	3.042	0.17	0.96	9.80
50	8.22	4.770	3.62	3.857	0.17	0.96	59.40
70	8.22	4.545	2.52	4.503	0.17	0.96	122.00
90	8.22	5.463	2.52	4.495	0.17	0.96	130.00
110	8.22	8.405	2.62	3.570	0.30	0.7	162.00

τ_F and τ_{HN} are the Fröhlich and Havriliak–Negami relaxation time, S_F and S_{HN} are the relaxation strength, α and β the relaxation parameters and σ is the conductivity.

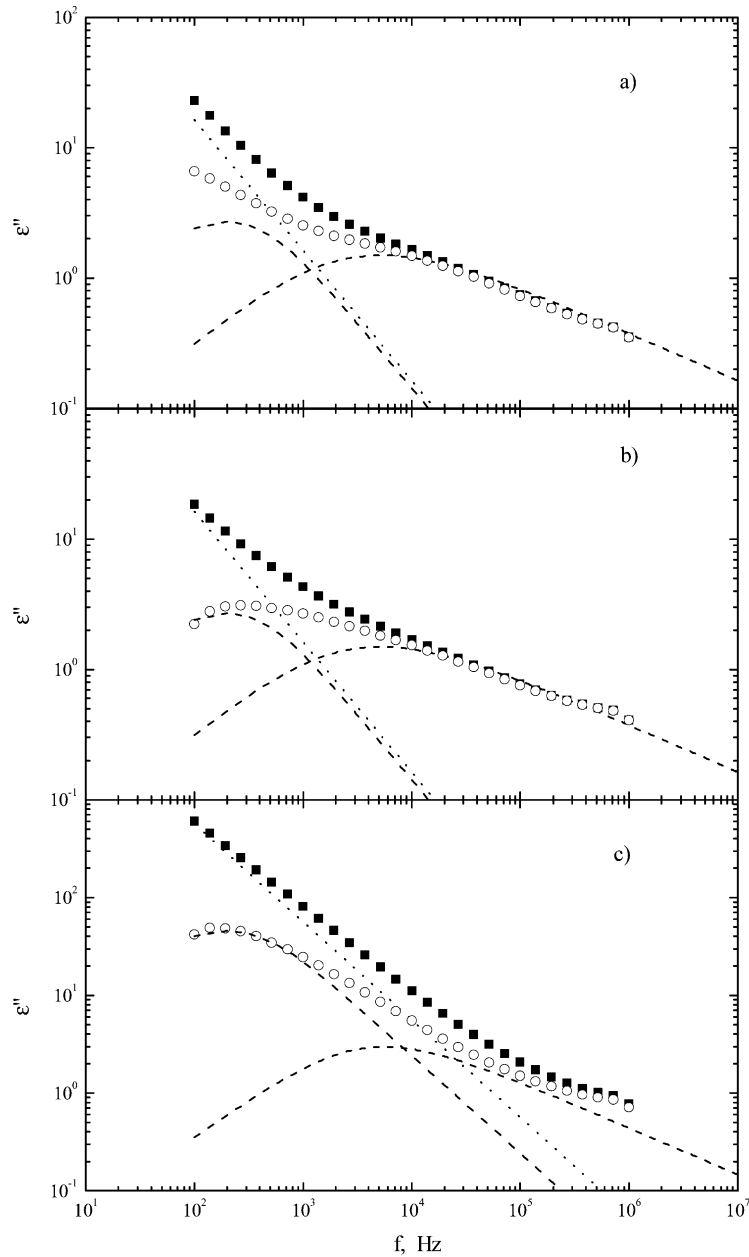


Fig. 5. Absorption curves of (a) 20%, (b) 50% and (c) 80% CS/PVA at 90 °C. The data are fitted by one Havriliak–Negami, one Fröhlich and conductivity term. (■) ϵ''_{exp} , (---) ϵ''_{HN} , (○) ϵ''_{theo} , (- - -) ϵ''_{F} , (···) ionic conductivity.

the applied agent but also by the bacterial species which the agent acts upon.

4. Conclusion

- The miscibility of chitosan blended with polyvinyl alcohol and polyvinyl pyrrolidone (CS/PVA and CS/PVP) with the different compositions in dilute solutions of 0.1 acetic acid/water were studied using viscosity technique based on Huggin's equation. The results obtained indicate that CS/PVA and CS/PVP are compatible.
- The dielectric data for such systems carried out at different frequencies ranging from 10^2 to 10^6 Hz indicated that more than one relaxation mechanism was present. These mechanisms which were detected using Fröhlich and/or Havriliak–Negami functions in addition to conductivity term are related to the rotation of the main chain and its related motions.
- The biological activities of the two investigated systems (CS/PVA and CS/PVP) were tested against a representative number of pathogenic organisms using minimum inhibitory concentration (MIC) method. It is found that the MIC for both systems decrease by increasing the

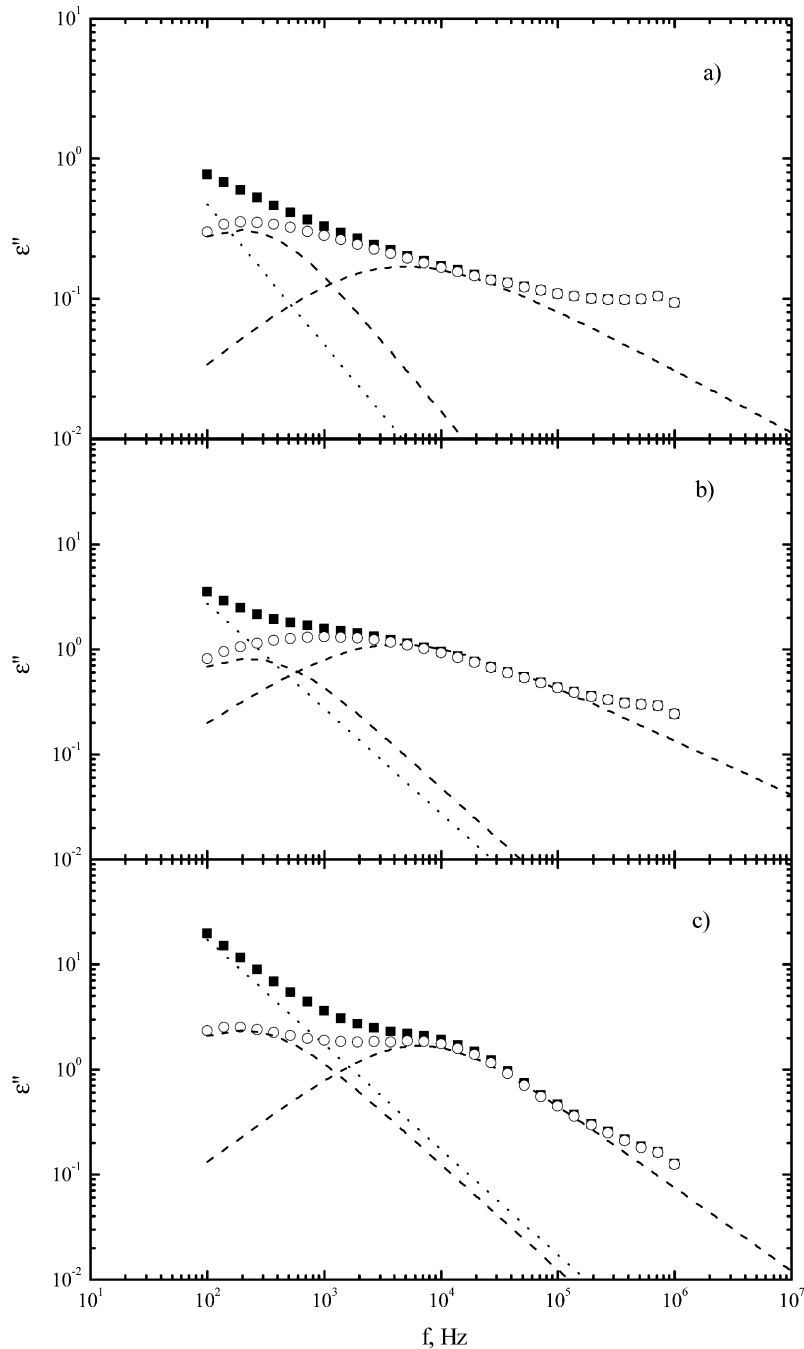


Fig. 6. Absorption curve of (a) 20%, (b) 50% and (c) 80% CS/PVP at 90 °C. The data are fitted by one Havreliak–Negami, one Fröhlich and conductivity term. (■) ϵ''_{exp} , (---) ϵ''_{HN} , (○) ϵ''_{theo} , (- · -) ϵ''_{F} , (···) ionic conductivity.

amount of CS in the blends, i.e. increase in the biological activity.

References

- [1] Ikejima T, Yagi K, Inoue Y. *Macromol Chem Phys* 1999;200(2):413.
- [2] Shigemasa Y, Minami S. *Chitin/chitosan, a handbook of chitin and chitosan*. Tokyo: Gihodo Publishing Co., Japan Soc.; 1995. p. 178.
- [3] Muzzarelli RAA. *Cell Mol Life Sci* 1997;53:137.
- [4] Zang Z, Kimura Y, Takahashi M, Yamane H. *Polymer* 2000;41(3):899.
- [5] Japanese Chitin and Chitosan Society. *Chitin and chitosan hand book*. Tokyo: Gihodo; 1995. p. 460.
- [6] Sakurai K, Maegowa T, Takahashi T. *Polymer* 2000;41(19):7051.
- [7] Ratto JA, Chien CC, Blumstein RB. *J Appl Polym Sci* 1996;59(9):1451–61.
- [8] Jiang WH, Han SJ. *J Polym Sci, Part B: Polym Phys* 1998;36(8):1275.
- [9] Niconovich GV, Burkhonova ND, Yunusor MY, Yugai SM, Milusheva RY. *Chem Nat Compd* 2000;36(3):258.
- [10] Fang L, Goh SH. *J Appl Polym Sci* 2000;76(12):1785.
- [11] Mucha M, Pieknielna J, Wiczorek A. *Macromol Symp* 1999;144:391.

- [12] Choung WY, Young TH, Chiu WY. *Biomaterials* 1999;20(16):1479.
- [13] Koyona T, Minoura N, Nagura M, Kobayoshi K. *J Biomed Mater Res* 1998;39(3):486–90.
- [14] Sato M, Koshino T, Kajitani Y, Inamura I, Kubo Y. *J Appl Polym Sci* 2004;93(4):1616–22.
- [15] Shieh JJ, Huang RYM. *J Membr Sci* 1997;127(2):185–202.
- [16] Haimovich B, Divazio L, Katz D, Zhang L, Greco RS, Dror Y, et al. *J Appl Polym Sci* 1997;63(11):1393–400.
- [17] Young ML, Su HK, Seon JK. *Polymer* 1996;37(26):5897–905.
- [18] Dufresne A, Cavaillé JY, Dupeyre D, Garcia-Ramirez M, Romero J. *Polymer* 1999;40(7):1657–66.
- [19] Cao S, Shi Y, Chen G. *Polym Bull* 1998;41(5):553–9.
- [20] Koyano T, Minoura N, Nagura M. *Kabunshi-Ronbunshu* 1998;55(6):305–13.
- [21] Guan YL, Liu XF, Fu QA, Li Z, Yao KD. *Carbohydr Polym* 1998;36(1):61–6.
- [22] Huggins ML. *J Am Chem Soc* 1942;64:2716.
- [23] Garcia R, Melad O, Gomez CM, Figueruelo JE, Compos A. *Eur Polym J* 1999;35(1):47–55.
- [24] Parada LG, Casteros LC, Meauria E, Katime I. *Polymer* 1998;39(5):1019–24.
- [25] Fröhlich H. *Theory of dielectrics*. 2nd ed. Oxford: Clarendon Press; 1958. p. 93.
- [26] Havriliak S, Negami S. *J Polym Sci* 1966;C14:99.
- [27] Wagner KW. *Arch Elektrotechnol* 1914;2:371.
- [28] Blythe AR. *Properties of polymers*. Solid state science series. Cambridge: Cambridge University Press; 1979.
- [29] Sakurai K, Maegawa T, Takahashi T. *Polymer* 2000;41(19):7051–6.
- [30] Lee YM, Kim SH, Kim SJ. *Polymer* 1996;37(26):5897.
- [31] Cendoya I, Lopez D, Alegria A, Mijangos C. *J Polym Sci, Part B: Polym Phys* 2001;39:1968–75.
- [32] Mubarak SIM, Sugdem JK. *Pharm Acta Helv* 1984;59:205.